

Arctic Sea Ice Classification Using Artificial Intelligence and NASA Team 2 Algorithm

Ji-Won Kim (1), Yang-Won Lee (2)

¹ Pukyong National Univ., 45 Yongso-ro, Nam-gu, Busan, Korea

² Pukyong National Univ., 45 Yongso-ro, Nam-gu, Busan, Korea

Email: ziwon@pukyong.ac.kr; modiconfi@pknu.ac.kr

KEY WORDS: AMSR2, sea ice classification, sea ice concentration, artificial intelligence

ABSTRACT: Sea ice plays an important role in keeping the polar regions cool and helping moderate global climate. The passive microwave sensors are widely used to estimate sea ice properties because it can penetrate clouds and detect sea ice during the day and night, regardless of cloud cover. The Advanced Microwave Sounding Radiometer2 (AMSR2) aboard the Global Change Observation Mission – Water1 (GCOM – W1) provides record of enhanced sea ice products with high spatial resolution and other improvements than previous several microwave sensors. Sea ice concentration from the AMSR2 is calculated by using NASA Team2 (NT2) sea ice algorithm known to calculate accurate sea ice concentration for the Arctic and Antarctic. The NT2 has been addressed some of the weaknesses of the NASA Team (NT) algorithm by employing high frequency 89 GHz channels unlike many other algorithms in order to consider sea ice with surface affect. Sea ice and open water are characterized by different brightness temperature depending on the wavelength. The NT2 calculates sea ice concentration using ratio based on these characteristics. In this study, we analyzed the radiation characteristics according to the sea ice type and open water in the Kara and Barents Seas through four ratios (PR , GR , PR_R , and ΔGR) used to distinguish the sea ice types in the NT2 algorithm. In addition, we propose the possibility of developing a classification and retrieval algorithm for sea ice by applying artificial intelligence to these radiation features.

1. Introduction

Sea ice, formed simply by freezing sea water, occurs mainly in the polar regions. However, sea ice not only keeps the polar regions cool, but also plays an important role in regulating the global climate by helping moderate global climate. Sea ice has a bright surface, so much of the sunlight that strikes it is reflected back into space. As a result, areas covered by sea ice don't absorb much solar energy, so temperatures in the polar regions remain relatively cool.

Remote sensing capabilities provide sea ice measurement and monitoring in difficult-to-access Arctic regions on a continuous basis and with much better spatial coverage than field or in situ measurements. Satellites can easily measure sea ice in the visible, infrared, and microwave regions of the electromagnetic spectrum. Among them, the passive microwave sensors compensate for the shortcomings of optical sensors that depend on weather and atmospheric conditions, and have the advantage of daily observation of the North and South poles (Cavalieri *et al.*, 1997). The Advanced Microwave Sounding Radiometer2 (AMSR2) aboard the Global Change Observation Mission – Water1 (GCOM – W1) provides record of enhanced sea ice products with high spatial resolution and other improvements than previous several microwave sensors. Sea ice concentration (SIC, the fraction of sea ice in a pixel) from the AMSR2 is calculated by using NASA Team2 (NT2) sea ice algorithm known to calculate accurate sea ice concentration for the Arctic and Antarctic. It improved the sea ice concentration error and spatial resolution of the NT algorithm used for SSM/I, and is known to produce an accurate sea ice concentration in the Arctic and Antarctic (Comiso *et al.*, 1997; Cavalieri *et al.*, 2006).

In this study, we analyzed the radiation characteristics according to the sea ice type and open water in the Kara and Barents Seas through four ratios (PR , GR , PR_R , and ΔGR) used to distinguish the sea ice types in the NT2 algorithm. In addition, we propose the possibility of developing a classification and retrieval algorithm for sea ice by applying artificial intelligence to these radiation

features.

2. Study Area and Data

2.1 Study Area

The National Snow and Ice Data Center (NSIDC) provides a region mask for the Arctic, which includes nine seas: The Seas of Okhotsk and Japan, Bering Sea, Hudson Bay, Baffin Bay/Davis Strait/Labrador Sea, Greenland Sea, Kara and Barents Seas, Arctic Ocean, Canadian Archipelago, and Gulf of St. Lawrence. We selected the Kara and Barents Seas as our study area, and grid points were extracted from the region mask (Figure 1). The Kara and Barents Seas represent a key area of Arctic sea ice shift (Yang *et al.*, 2016) as warm Atlantic waters flow into the Arctic Ocean (Sorteberg and Kvingedal, 2006).



Figure 1. Map of the study area.

2.2 Data

We used the AMSR-E/AMSR2 unified L3 (level-3) dataset of passive microwave brightness temperature provided by the NSIDC. This data set includes six daily brightness temperature fields for channels ranging from 6.9 through 89.0 GHz, three daily sea ice concentration fields, and three daily sea ice concentration difference fields for ascending orbits, descending orbits, and full orbit daily averages. All fields are mapped to 25 km polar stereographic projection. This product uses the Japan Aerospace Exploration Agency (JAXA) AMSR2 Level-1R input brightness temperatures that are calibrated, or unified, across the JAXA AMSR-E and JAXA AMSR2 Level-1R products. In this dataset, we used daily average brightness temperature data for 18.7, 36.5, and 89.0 GHz channels.

3. Method

3.1 NASA Team2 Sea Ice Algorithm

The microwave sensor distinguishes open water from ice-covered water by using radiative properties that represent a wide contrast between the emissivity of sea and sea ice (Figure 2). For sea ice observation, the 36 and 18 GHz horizontal and vertical (0.81 and 1.7 cm) are mainly used. These six spectra show two important characteristics: (1) the small polarization of either ice type compared to that of the ocean. (2) discrimination between ice types increases with decreasing wavelength and is greatest at the 0.81 cm wavelength (Cavalieri *et al.*, 1984).

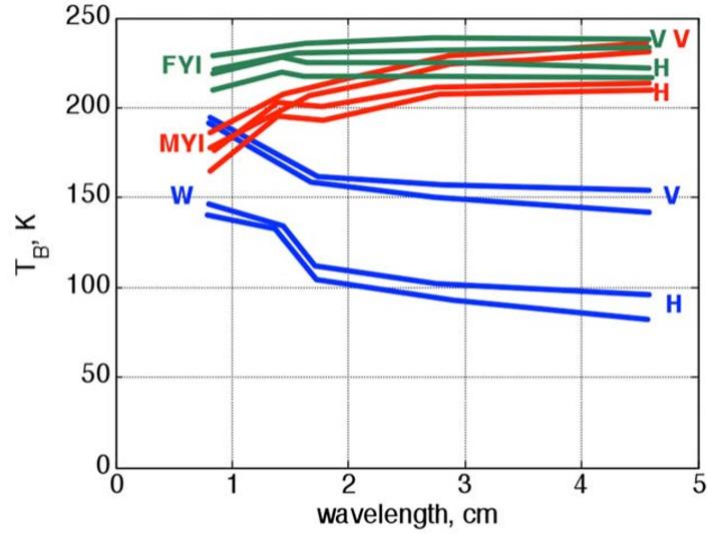


Figure 2. Microwave brightness temperatures of first-year ice, multi-year ice and open water according to wavelength. Sea Ice Concentration Algorithm Theoretical Basis Document, by European Space Agency, September 22 2017, Copyright 2017 by European Space Agency.

Based on these characteristics, the NT2 algorithm calculates PR , GR , PR_R , and ΔGR to classify the types of Arctic sea ice into first-year ice, multi-year ice, and ice type C, and to distinguish open water. Defined in terms of observed brightness temperatures T_B in each channel (v) and polarization (p), PR and GR are calculated as

$$PR(v) = \frac{(T_B(v, V) + T_B(v, H))}{(T_B(v, V) + T_B(v, H))} \quad (1)$$

$$GR(v_1 p v_2 p) = \frac{(T_B(v_1 p) - T_B(v_2 p))}{(T_B(v_1 p) + T_B(v_2 p))} \quad (2)$$

$PR(18)$ and $GR(36V18V)$ calculated from Equations (1) and (2) serve as important variables to distinguish the type of sea ice and open water (Han and Lee, 2011). Multi-year ice and first-year ice are small values for these two ratios and relatively high at open water. However, in the case of ice type C where surface effects such as snow layers affect the radiation characteristics on the surface of the sea ice, $PR(18)$ value is as close as open water, and $GR(36V18V)$ maintains its value between multi-year ice and first-year ice (Andersen et al., 2007; Markus and Cavalieri, 2000). Ice with a high $PR(18)$ value often occurs when thick snow of more than 30 cm is piled on the ice or water is accumulated on the sea ice surface. Since the 89.0 GHz channel has the advantage of less surface influence than the data obtained at the 18 GHz horizontal, the NT2 algorithm used an 89.0 GHz vertical and horizontal in addition to the 18 and 36 GHz used in existing algorithm to calculate new variables called PR_R , and ΔGR . When ϕ is given by -0.18 radians for 18 GHz and -0.06 radians for 89 GHz in the Arctic, $PR_R(v)$ is calculated as

$$PR_R(v) = -GR(37V18V)\sin\phi + PR(v)\cos\phi \quad (3)$$

The greater the surface effect of sea ice (ice type C), the greater the value of $PR_R(18)$, but the $PR_R(18)$ is not as close to open water as $PR(18)$. In addition, the $PR_R(89)$ maintains a constant value close to zero even if the surface effect of the sea ice increases.

Using ΔGR , the ratio difference between 89.0 and 18.7 GHz vertical and horizontal, solves the problem of sensitivity, and further considers ice type C. The GRs (ΔGR) is calculated as

$$\Delta GR = GR(89H18H) - GR(89V18V) \quad (4)$$

However, 89.0 GHz has the disadvantage of being sensitive to atmospheric effects. Since the atmospheric conditions of the polar are always changing, the sensitivity of the 89.0 GHz channel also changes, so the NASA Team2 algorithm used a calibration model for various atmospheric conditions.

4. Results and Conclusion

We extracted the pixels corresponding to the Kara and Barents seas from the brightness temperature of 18.7, 36.5, and 89.0 GHz channels using the region mask provided by NSIDC. In addition, PR , GR , PR_R , and ΔGR were calculated to verify the sea ice and the radiative characteristics of open water in the Kara and Barents Seas. We compared radiative characteristics using data from April, when the oceans were mostly frozen, and September, when most sea ice was melting. Figure 3 shows the scatter plot between $PR(18)$ and $GR(36V18V)$, (a) and (b) using data from September, and (c) and (d) using April data. As a result, in September when most of the sea ice melts, it can be seen that there are many pixels with high values of $PR(18)$ and $GR(36V18V)$. On the other hand, in April, when the sea ice is frozen, it can be seen that $PR(18)$ and $GR(36V18V)$ form clusters at relatively low values. In addition, plots ((b) and (d)) between $GR(89H18H)$ and $GR(89V18V)$ using the 89.0 GHz channel show radiation characteristics between open water and sea ice. Based on the characteristics of forming clusters according to sea ice and open water, this study intends to classify by sea ice type and open water using artificial intelligence method.

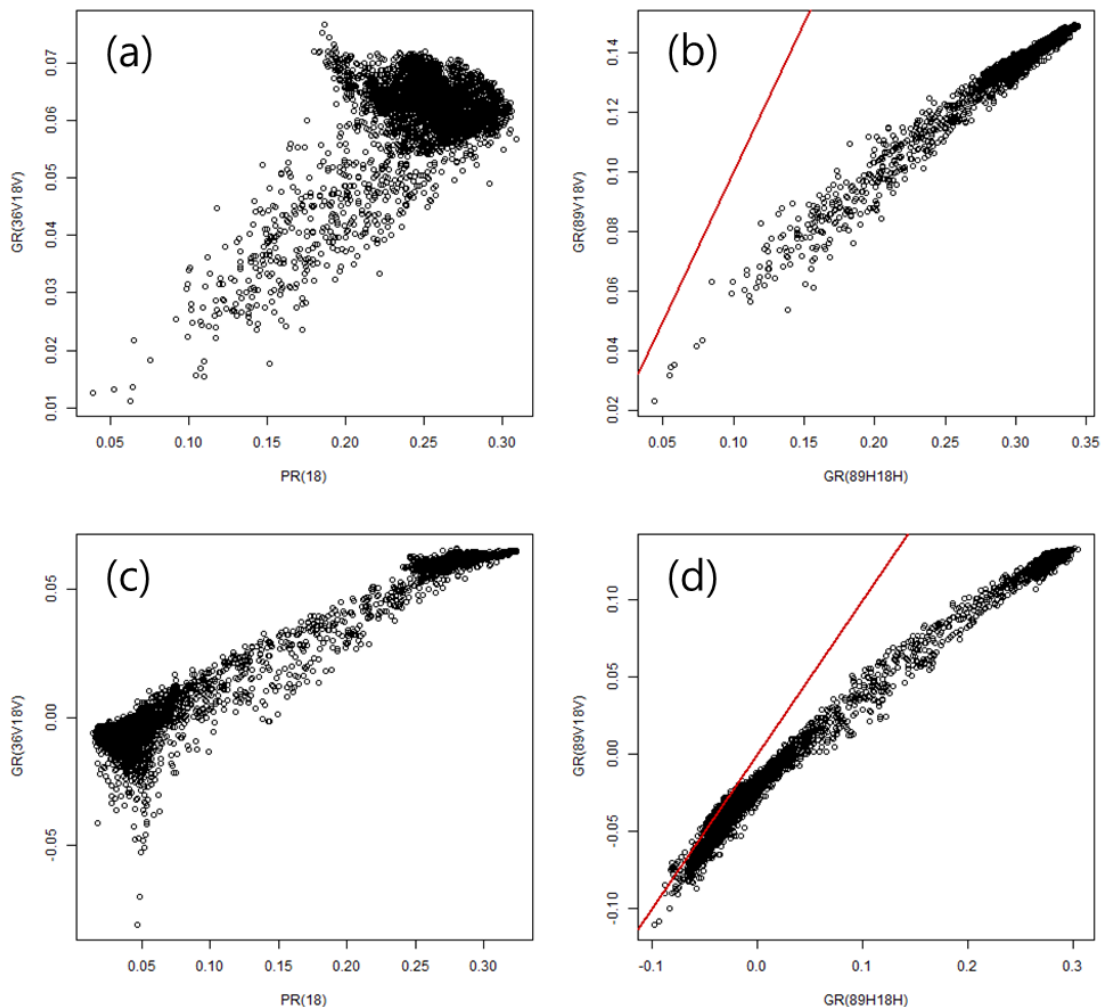


Figure 3 (a) and (b): $PR(18)$ versus $GR(36V18V)$ and $GR(89H18H)$ versus $GR(89V18V)$ for the Kara and Barents Seas on September 1, 2012. (c) and (d): $PR(18)$ versus $GR(36V18V)$ and $GR(89H18H)$ versus $GR(89V18V)$ for the Kara and Barents Seas on April 1, 2012.

References

- Andersen, S., L. Kaleschke, G. Heygster, and L.T. Pedersen, 2007. Intercomparison of passive microwave sea ice concentration retrievals over the high-concentration Arctic sea ice, *Journal of Geophysical Research*, 112, C08004.
- Cavalieri, D. J., Gloersen, P., Campbell, W. J. 1984. Determination of sea ice parameters with the NIMBUS 7 SMMR. *Journal of Geophysical Research: Atmospheres*, 89(D4), 5355-5369.
- Cavalieri, D.J., P. Gloersen, C.L. Parkinson, J.C. Comiso, and H.J. Zwally, 1997. Observed hemispheric asymmetry in global sea ice changes, *Science*, 278(5340): 1104-1106.
- Cavalieri, D.J., T. Markus, D.K. Hall, A.J. Gasiewski, M. Klein, and A. Ivanoff, 2006. Assessment of EOS Aqua AMSR-E arctic sea ice concentration using Landsat-7 and airborne microwave imagery, *IEEE Transactions on Geoscience and Remote Sensing*, 44(11): 3057-3069.
- Comiso, J.C., D.J. Cavalieri, C.L. Parkinson, and P. Gloersen, 1997. Passive microwave algorithms for sea ice concentration: A comparison of two techniques, *Remote Sensing of Environment*, 60(3): 357-384.
- European Space Agency (ESA). Sea Ice Concentration Algorithm Theoretical Basis Document (ATBD). pp. 25. Available online: http://cci.esa.int/sites/default/files/SeaIce_CCI_P2_ATBD_D2.1__SIC__Issue_1.0.pdf
- Han, H.S, Lee, H.Y. 2011. Microwave Radiation Characteristics of Glacial Ice in the AMSR-E NASA Team2 Algorithm. *Korean Journal of Remote Sensing*, 27(5), 543-553.
- Markus, T., D.J. Cavalieri, A.J. Gasiewski, M. Klein, J.A. Maslanik, D.C. Powell, B.B. Stankov, J.C. Stroeve, and M. Sturm, 2006. Microwave signatures of snow on sea ice: Observations, *IEEE Transactions on Geoscience and Remote Sensing*, 44(11): 3081-3090
- Sorteberg, A., Kvingedal, B., 2006. Atmospheric forcing on the Barents Sea winter ice extent. *Journal of Climate*, 19(19), 4772-4784.
- Yang, X.Y., Yuan, X., Ting, M., 2016, Dynamical link between the Barents–Kara sea ice and the Arctic Oscillation. *J. Clim.* 29, 5103–5122.